Chapter 5

Lipid Raft-Redox Signaling Platforms in Plasma Membrane

Fan Yi, Si Jin, and Pin-Lan Li

Summary

Membrane lipid rafts (LRs) have been demonstrated to be importantly involved in transmembrane signaling in a variety of mammalian cells. Many receptors can be aggregated within the LR clusters to form signaling platforms. Currently, LRs were reported to be clustered to aggregate, recruit, and assemble NADPH oxidase subunits and related proteins in various cells in response to various stimuli, forming redox signaling platforms. These LR signaling platforms may play important roles in the regulation of cellular activity and cell function, and also in the development of cell dysfunction or injury associated with various pathological stimuli. This LRs clustering-mediated mechanism is considered to take a center stage in redox signaling associated with death receptors. In this chapter, some basic methods and procedures for characterization of LR-redox signaling platforms formation and for determination of the function of these signaling platforms are described in detail, which include identification of LR-redox signaling platforms in cell membrane by using fluorescent or confocal microscopy of LR-redox signaling platforms and fluorescent resonance energy transfer analysis, isolation of LR-redox signaling platforms by flotation of detergent-resistant membranes, and function measurement of LR-redox signaling platforms by electron spin resonance spectroscopy. It is expected that information provided here will help readers to design necessary experiments in their studies on LR signaling platforms and redox regulation of cell function.

Key words: Lipid microdomains, Reactive oxygen species, Molecular trafficking, Sphingolipids

1. Introduction

There is increasing evidence that clustering of distinct cholesterol- and sphingolipid-rich membrane microdomains or lipid rafts (LRs) is importantly involved in transmembrane signaling in a variety of mammalian cells. Many receptors including tumor necrosis factor-α receptors, Fas, DR3, -4, -5, insulin receptors, and integrins as well as other postreceptor signaling molecules may

Donald Armstrong (ed.), *Lipidomics,* Methods in Molecular Biology, vol. 580,
DOI 10.1007/978-1-60761-325-1_5,

be aggregated within the LR clusters to form signaling platforms *(1, 2)*. It has been indicated that LRs clustering or platform formation is implicated in the regulation of a number of biological processes in different cells including cell growth, differentiation and apoptosis, T-cell activation, tumor metastasis, neutrophil and monocyte infiltration, as well as infection of different pathogen organisms such as bacteria, viruses, and parasites *(3)*. Among different LRs, a ceramide-enriched membrane platform has been extensively studied. Evidence is increasingly accumulated that this ceramide-enriched membrane platform plays an essential role in the regulation of cellular signaling. The mechanism mediating this cellular signaling is associated with establishment of a proximity of many receptor molecules, facilitation of transactivation of signaling molecules associating or interacting with a receptor, and amplification of the specific signaling of the activated receptors *(4, 5)*. Therefore, this ceramide-enriched membrane platform is also referred as to LR signaling platform. It has been established that the formation of the LR signaling platforms with aggregation of different signaling molecules is an important mechanism, determining the variety of transmembrane signaling that could robustly amplify signals from activated receptors on the cell membrane *(6, 7)*.

Studies in our laboratory and by others have reported that in response to different stimuli such as activation of death receptors, carcinogenic factors, and degenerative stimuli LRs may be clustered due to ceramide production by activation acid sphingomyelinase, where various redox molecules like superoxide ($O_2^{\cdot-}$), H_2O_2, or peroxinitrite ($ONOO^-$) can be produced. It has been demonstrated that in ceramide-enriched membrane domains or platforms, different enzymes or factors associated with production or metabolism of redox molecules are clustered by translocation, recruitment, or aggregation such as NADPH oxidase, $O_2^{\cdot-}$ dismutase, and thioreductase *(8, 9)*. Since this LR platform produces redox molecules in response to different stimuli and thus regulates cellular activity or cell function, it is now called the LR-redox signaling platform. In this regard, the NADPH oxidase subunits have been demonstrated to be clustered with ceramide-enriched membrane domains, and this LR clustering-mediated redox signaling has been commented as taking center stage in signaling of death receptors *(10)*. This LR clustering mechanism may provide a driving force to cause NADPH oxidase assembling and activation.

It is well know that NADPH oxidase is a multicomponent enzyme complex that consists of the membrane-bound cytochrome b_{558} (gp91^{phox} and p22^{phox}) and cytoplasmic proteins (p40^{phox}, p47^{phox}, p67^{phox}, and Rac GTPase) that translocate to the membrane to form an assembled complex following cellular stimulation to

produce $O_2^{\bullet-}$. The $p47^{phox}$ translocation is considered as a key step, to some extent, a marker event, for the assembly and activation of NADPH oxidase, which is assumed to be initiated by the phosphorylation of this subunit at various phosphorylation sites by PKC, PKA, or MAPK *(11)*. In addition, the catalytic subunits of this enzyme are termed NOX proteins, which include several known members, namely, NOX1, NOX2 ($gp91^{phox}$), NOX3, NOX4, and NOX5, DUOX1, and DUOX2 *(12)*. However, for a long time, it is unknown what is the precise mechanism that drive $p47^{phox}$ translocation and subsequent assembly of other NADPH oxidase subunits so efficiently in the cell membrane *(13, 14)*. Demonstration of LRs clustering of these NADPH oxidase may shift a paradigm in understanding the activation of NADPH oxidase and redox signaling *(8, 15–17)*.

In this chapter, the methods and procedures for characterization of LR-redox signaling platform formation and related protocols for functional studies of LR signaling platforms are described in detail. These basic procedures and methods include identification of LR-redox signaling platforms in cell membrane by using fluorescent or confocal microscopy of LR-redox signaling platforms and fluorescent resonance energy transfer (FRET) analysis, isolation of LR-redox signaling platforms by flotation of detergent-resistant membranes (DRMs), and function measurement of LR-redox signaling platforms by electron spin resonance (ESR) spectroscopy. The authors hope that these protocols would help readers design experiment to understand the physiological or pathological relevance of LR-redox signaling platforms, to explore the molecular mechanisms underlying the formation of LR-redox signaling platforms, and to develop new therapeutic strategies for treatment of diseases or pathological processes related to this LR signaling platform.

It should be noted that besides these methods in this chapter, other general visualization techniques for LRs may also be used for further studies on such LR-redox signaling platforms. For example, total internal reflection microscopy allows us to get information of the diffusivity of particles in the membrane as well as to reveal membrane corrals, barriers, and sites of confinement. Fluorescence correlation and cross-correlation spectroscopy can be used to gain information of fluorophore mobility in the membrane. In addition, atomic force microscopy, scanning ion conductance microscopy, nuclear magnetic resonance, and superresolution microscopy such as stimulated emission depletion may also be used, if related equipment or instruments are available. **Figure 1a** summarizes all commonly used methods for studies of LRs or LR-redox signaling platforms. The rationales of methods that we introduce in this chapter are described in following text.

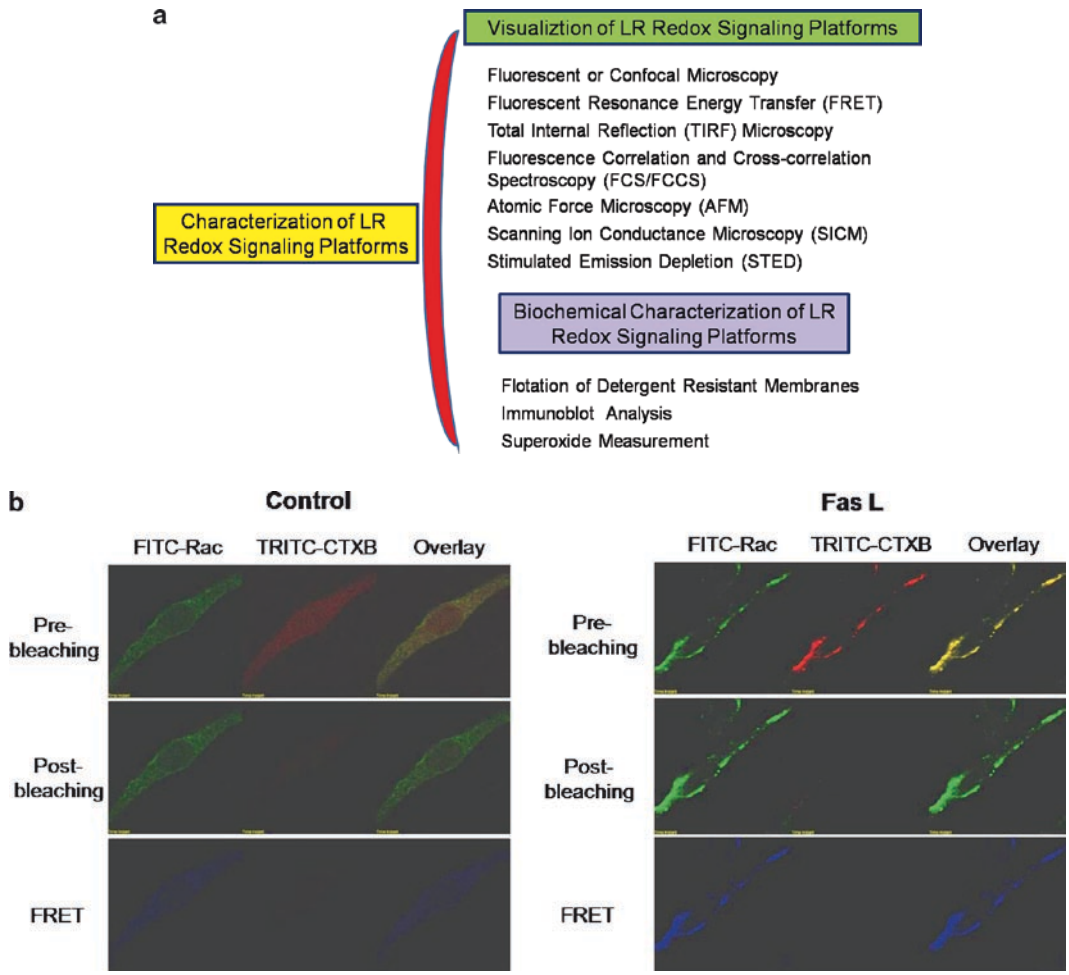

Fig. 1. Characterization of lipid raft redox signaling platforms in plasma membrane. (**a**) Methods commonly used to characterize of the formation of lipid raft redox signaling platforms. (**b**) Representative images of FRET analysis between FITC-Rac1 and TRITC-CTXB in BCAECs. The left group of images shows a control cell costained with FITC-Rac1 and TRITC-CTXB that underwent an acceptor bleaching protocol. Both the pre- and postbleaching images were presented on the top and middle panels. FRET image (in blue) was generated by subtraction of fluorescent intensity in the prebleaching image from that in the postbleaching image of FITC-Rac1 labeling. As shown in FRET image (blue in the *bottom image*), there was very low FRET detected under control condition. The right group of images shows a FasL-stimulated cell that underwent the same FRET protocol. In addition to detected patch formation (lipid raft clustering and Rac aggregation) and colocalization of both molecules seen in the overlaid images (*top panel*) in response to FasL, a more intense FRET image (blue one in the *bottom*) was detected in this FasL-treated BCAEC, demonstrating that energy transfer occurs between a Rac1 and LR component-GM1 ganglioside.

1.1. Identification of LR-Redox Signaling Platforms in Cell Membrane: Fluorescent or Confocal Microscopy and FRET Analysis

These methods are used to detect a colocalization of LRs components and aggregated or recruited NADPH oxidase subunits or other molecules related to redox signaling on the cell membrane. Although individual LRs are too small to be resolved on the cell surface by standard light microscopy, clustered LRs could be visualized by fluorescence or other staining techniques if their components are cross-linked with antibodies or lectins. Therefore, fluorescent or confocal microscopy of LR patches or

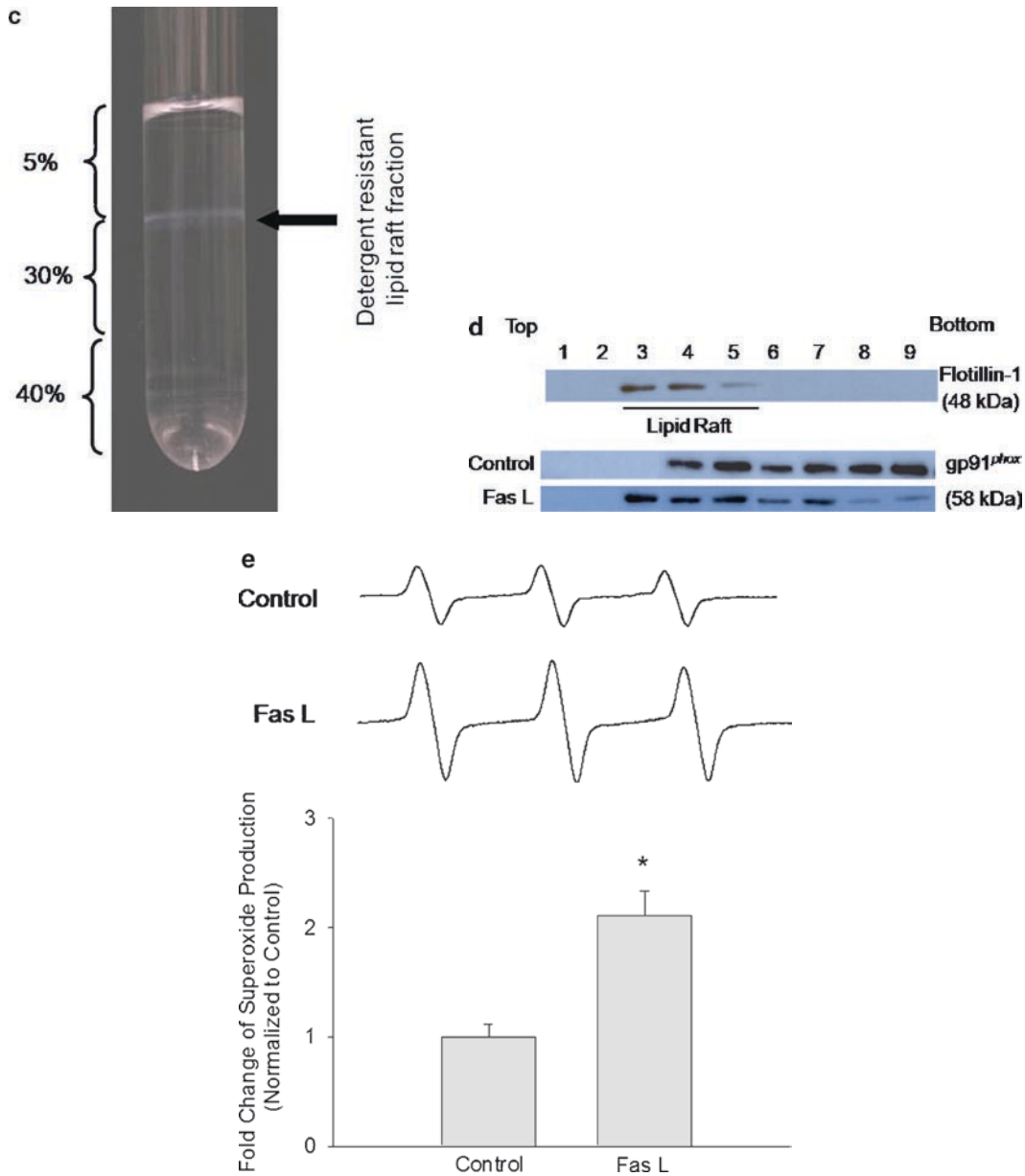

Fig. 1. (continued) (**c**) Isolation of detergent-resistant lipid raft fractions from BCAECs based on their detergent insolubility and low density. (**d**) After density gradient ultracentrifugation, nine fractions from top to bottom were fractionated and then analyzed by immunoblotting. Fractions #3–5 were designated as LRs indicated by flotillin-1 (one marker for lipid rafts). The blot pattern for gp91^{phox} indicated that gp91^{phox} subunit was aggregated to membrane lipid raft fractions of FasL-treated BCAECs. (**e**) Representative ESR spectra showing SOD-inhibitable $O_2^{\cdot-}$ signals (*upper*) and summarized data depicting $O_2^{\cdot-}$ production indicating that FasL significantly increased $O_2^{\cdot-}$ production in lipid raft fractions.

spots on the cell membrane is widely used as a common method currently. One of LRs markers is fluorescent labeled-cholera toxin (CTX), which is used based on its capacity of binding to the raft constituent ganglioside GM_1, a glycosphingolipid that consists of a ceramide backbone with four sugars esterified, one of these

being N-acetylneuraminic acid, galactose, and glucose *(18)*. Since this LR signaling platform is ceramide-enriched domain, ceramide can also be used as a marker to detect this LR signaling platform or ceramide-enriched microdomains by fluorescent or confocal microscopy.

The current advances in fluorescence microscopy, coupled with the development of new fluorescent probes, make FRET analysis widely being used as a powerful technique for studying molecular interactions in cells. This analysis will reveal molecular proximity of various molecules in a variety of cells with improved spatial (angstrom) and temporal (nanosecond) resolution, distance range, and sensitivity as well as a broader range of biological applications *(19)*. FRET is a phenomenon that occurs between a fluorophore pair, donor and acceptor (e.g., FITC and TRITC). The fluorophore pair shares the character that the emission wavelength of the donor can overlap with the excitation wavelength of the acceptor, in which energy can transfer from the donor to the acceptor. Two key factors determine the occurrence of FRET, molecular orientation and distance between the molecules. It is proposed that FRET can only take place between two molecules within 7–10 nm range. Detected FRET generally indicates that the two molecules are closely located, which may generate energy transfer to each other or interact to lead to molecular reaction. Here we present some methods specific to detect FRET between LR components and redox producing or regulatory enzymes, in particular NADPH oxidase subunits and GM_1.

1.2. Isolation and Analysis of LR-Redox Signaling Platforms: Flotation of DRMs

This method is used to identify redox signaling molecules or other associated proteins and receptors in isolated LRs fractions. DRM complex or detergent-insoluble glycolipid-enriched domains (DIG) can float to low-density fractions during sucrose gradient centrifugation. These LR fractions are rich in raft proteins and therefore analyzing the raft proteins in DRM provides a reliable and simple means of identifying possible LR components, especially LRs-associated proteins *(2, 4, 20)*. Furthermore, in combination with proteomic techniques developed recently, this membrane flotation technique can help demonstrate all unidentified molecules including receptors, enzymes, and adaptors if large-scale proteomic analyses could reach enough resolutions and sensitivity. Currently, only some targeted proteomic analysis can be done given technical limitations *(21)*.

1.3. Functional Measurement of LR-Redox Signaling Platforms: ESR Spectroscopy

Among methods to characterize the activity and modulation of redox molecules or redox-related enzyme activity such as NADPH oxidase including lucigenin-enhanced chemiluminescence, dihydroethidium (DHE) fluorescent spectrometric assay, HPLC analyses, fluorescent dye intracellular trapping detection, and ESR, the most direct and definitive method is ESR spectrometric analysis. ESR, also called electron paramagnetic resonance spectroscopy, is

a technique for studying chemical species that have one or more unpaired electrons, such as organic and inorganic free radicals or inorganic complexes possessing a transition metal ion. ROS are often free radicals with unpaired electrons. Because they are very short-lived, it has been challenging to measure ROS from biological samples. The recently developed ESR has made highly specific, quantitative and reproducible measurements of ROS possible. Now ESR is commonly used for measurements of nitric oxide, $O_2^{\cdot -}$, and other ROS from live cells, organelles, and tissues *(16, 22)*.

2. Materials

2.1. Equipment

1. Centrifuge (.maximum force ~17,000 × *g*).
2. The Optima™ Series ultracentrifuges and related rotors (Beckman, Fullerton, CA).
3. Olympus FV-300 FluoView Confocal Microscope Workstation (Shinjuku-kuTokyo, Japan) or Leica TCS-SP2 AOBS inverted confocal laser scanning microscope and workstation (Wetzlar, Germany).
4. Miniscope 200 ESR spectrophotometer (Magnettech, Berlin, Germany).

2.2. Reagents

2.2.1. Cell Culture

1. RPMI 1640 medium supplemented with 15% (v/v) fetal bovine serum, 1% antibiotic solution (Invitrogen, Carlsbad, CA).
2. Sterile phosphate-buffered saline (PBS) solution, pH = 7.4 (Sigma, St. Louis, MO).
3. 0.25% Trypsin-EDTA (Invitrogen, Carlsbad, CA).

2.2.2. Slide Preparations

1. Alexa Fluor 488-conjugated CTX B subunit (Molecular Probes, Carlsbad, CA) or anti-ceramide antibody (Alexis Biochemicals, Farmingdale, NY).
2. gp91^{phox} monoclonal antibody (BD Bioscience, San Jose, CA) or other related antibodies for NADPH oxidase subunits.
3. Texas Red-conjugated anti-mouse secondary antibody (Santa Cruz, Santa Cruz, CA).
4. 4% Paraformaldehyde (PFA) solution in PBS (*see* **Note 1**).
5. 100 ml 0.05% (v/v) Tween-20 in PBS (PBT).
6. 10 ml 1% (w/v) BSA in PBT.
7. 20 ml 0.1% BSA in PBT (diluted from 1% (w/v) BSA in PBT).
8. All conjugated, primary, and secondary antibodies diluted in 0.1% BSA in PBT.
9. Vectashield Mounting Media (Vector Labs, Burlingame, CA).

2.2.3. FRET Analysis

1. TRITC-conjugated CTX B subunit (acceptor).
2. FITC-labeled primary antibodies (donor).
3. TRITC-anti-mouse-IgG (as positive control).

2.2.4. Flotation of DRMs

1. MES-buffered saline (MBS) buffer**:** 25-mM 2-(*N*-morpholino) ethanesulphonic acid (MES), 150-mM NaCl, and 1-mM EDTA, pH = 7.4.
2. Triton X-100 detergent (Sigma, St. Louis, MO).
3. 60% OptiPrep® density gradient medium (Sigma, St. Louis, MO) (*see* **Note 2**).
4. Phenylmethylsulfonyl fluoride (Roche, Branchburg, NJ).
5. Na_3VO_4 (Sigma, St. Louis, MO).
6. One tablet "complete" protease inhibitors dissolved in 1-ml dH_2O (Roche, Branchburg, NJ)
7. MBS buffer containing 1-mM Na_3VO_4, 1-mM phenylmethylsulfonyl fluoride, and "complete" protease inhibitors (1:50 dilution) (solution A).
8. Solution A containing 1% (v/v) Triton X-100 (solution B) (*see* **Note 3**).
9. Thirty percent and 5% density gradient solutions: Dilute the Optiprep density gradient medium (60%) 1:1 and 1:11 in solution A for 30% and 5% solutions, respectively.

2.2.5. Superoxide Measurement by ESR

1. 10-mM 1-hydroxy-3-methoxycarbonyl-2,2,5,5-tetramethylpyrrolidine (CMH) (Noxygen, Elzach, Germany) (*see* **Note 4**).
2. Polyethylene glycol superoxide dismutase (PEG-SOD; 1000 U/ml) (Sigma, St. Louis, MO).
3. Diethyldithiocarbamate (DETC) (Sigma, St. Louis, MO).
4. Deferoamine (Sigma, St. Louis, MO).
5. Kreb/HEPES buffer (KHB).
6. Modified Kreb's/HEPEs buffer (containing 25 μM deferoxamine and 5 μM DETC) (*see* **Note 5**).
7. 10-mM CMH in modified Kreb's/HEPEs buffer.

3. Methods

3.1. Confocal Microscopy

1. On day 1, plate Bovine coronary arterial endothelial cells (BCAECs) in T-75 flasks at 5×10^6 cells/flask (*see* **Note 6**).
2. On day 2, split and plate cells at about 70% confluence on a four-chamber glass slide in fresh medium for at least 2 h at 37°C (*see* **Note 7**).

3. Add stimuli such as FasL (final concentration is 10 ng/ml) to treat cells for 15 min.
4. Aspirate medium and wash each chamber twice quickly with 0.5 ml PBS.
5. Fix the cells by adding 0.5 ml of 4% PFA to each chamber and incubating for 15 min.
6. Wash cells in PBT three times (each time for 5 min) on the shaker and then incubate cells for 30 min in 0.5 ml of 1% BSA.
7. Wash cells in PBT three times (each time for 5 min) on the shaker and then incubate cells in 0.5 ml of the working concentration of anti-gp91 antibody diluted in 0.1% BSA for 1 h.
8. Repeat step 7 using Texas Red-conjugated anti-mouse secondary antibody working solution (*see* **Note 8**).
9. Repeat step 7 using the Alexa 488-conjugated CTX working solution (*see* **Note 9**).
10. Wash cells in PBT three times (each time for 5 min) on the shaker.
11. Allow the slide to dry and remove the plastic chamber piece and sealer holding in place completely.
12. Place one drop of Vectashield Mounting Media on each sheet of cells and cover with a No. 1.5 thickness coverslip (Warner Instruments, Hamden, CT). Gently push out any air bubbles that form underneath the coverslip and seal the edges with clear nail polish.
13. Store slides at 4°C in the dark before and during viewing under fluorescence.
14. Staining is visualized using a conventional fluorescence microscope or a Leica TCS SP2 scanning confocal microscope (*see* **Note 10**).

3.2. FRET Analysis

1. Same procedures as steps 1–6 in **Subheading 3.1**.
2. Wash cells in PBT three times (each time for 5 min) on the shaker and then incubate cells in 0.5 ml of the working concentration of the FITC-conjugated donor antibody diluted in 0.1% BSA for 1 h.
3. Repeat step 2 using the TRITC-conjugated acceptor antibody.
4. Same procedures as steps 10–13 in **subheading 3.1**.
5. Capture digital images of donor, acceptor, and FRET fluorescent patterns (*see* **Note 11**).
6. Effectively and irreversibly bleach acceptor fluorescence by continuous excitation for 2 min at the acceptor wavelength.
7. Capture digital images of donor, acceptor, and FRET fluorescent patterns after bleaching.

8. FRET images are obtained by the subtraction of the prebleaching images from the postbleaching images (*see* **Note 12**).

3.3. Flotation of DRMs

1. Culture BCAECs in 10 cm^2 dishes at 5×10^6 cells/dish.
2. Aspirate medium. Culture cells with fresh medium. Then treat BCAECs with or without FasL (10 ng/ml, 15 min, Upstate, Billerica, MA).
3. Wash each dish three times in cold PBS, aspirate PBS, and then add 1 ml PBS to scrape the cells using a rubber, flexible scraper, transfer cells of each dish into 1.7 ml eppendorf tube individually.
4. Centrifuge the cell suspension at 3,000 × *g* for 5 min and discard the supernatant.
5. Resuspend cell pellets in 1 ml solution B (*see* **Note 13**)
6. Homogenize cell extracts by 10–15 passages through a 25-gauge needle and then incubate 60 min on ice.
7. Dilute each sample to 1.5 ml by adding the appropriate amount of solution B. Combine this with 3 ml 60% density gradient solution and mix well by pipetting up and down. Transfer this mixture (final including 40% density gradient solution) to a Beckman ultracentrifuge tube.
8. Add 4.5 ml 30% density gradient solution carefully to the ultracentrifuge tube, not disturbing the barrier between this and the solution already sitting in the tube (*see* **Note 14**).
9. Add 4.5 ml 5% density gradient solution carefully to the centrifuge tube, not disturbing the barrier between this and the solution already sitting in the tube.
10. Equalize the masses of all samples by weighing and identifying the heaviest sample, then adding dropwise 5% density gradient solution to the others so that all masses are exactly equal.
11. Spin in a Beckman SW 32 Ti rotor ultracentrifuge at 32,000 rpm at 4°C for 20 h (*see* **Note 15**).
12. Remove each sample from the ultracentrifuge and, by pipetting from the very top of the sample, aliquot the whole sample into nine 1.5 ml fractions in 1.7 ml ependorff tubes. Nine fractions are collected from the top to the bottom (fraction numbers 1–9) (*see* **Note 16**). Store samples in –80°C until ready to proceed.
13. For immunodetection of LR-associated proteins, 30 μl of each fraction (see **Note 17**) are subjected to SDS-PAGE, transferred onto a nitrocellulose membrane, and prepared for Western blot analysis using related antibodies such as LR marker flotinllin-1 and NADPH oxidase subunits ($p47^{phox}$, $p67^{phox}$, $gp91^{phox}$, and Rac GTPase et. al) (see **Note 18**).

14. Analysis: All films with immunoreactive blots are scanned by a densitometer and the intensity of corresponding protein bands was quantitated using UN-SCAN-IT software (Silk Scientific Corporation, Orem, Utah).

3.4. Superoxide Measurement by ESR Spectroscopy

1. LR isolation and identification (*see* **Subheading 3.3**).
2. Add 10 μl 10 mM CMH to 90 μl modified Kreb's/HEPEs buffer and incubate for 10 min (*see* **Note 19**).
3. 50 μl from step 2 is transferred to a 50-μl capillary tube and analyzed in an ESR spectrometer by time scan to quantify $O_2^{\cdot -}$ (*see* **Note 20**).
4. Incubate 20 μg LR fractions and 10 μl 3mM NADPH in modified Kreb's/HEPEs buffer for 10 min (total volume is adjusted to 90 μl using Kreb's/HEPEs buffer) (*see* **Note 21**).
5. After incubation, add 10 μl 10 mM CMH to 90 μl reaction mixture from step **4**.
6. 50 μl from step 5 is transferred to a 50 μl capillary tube immediately and analyzed in an ESR spectrometer by time scan to quantify $O_2^{\cdot -}$.
7. Incubate 20 μg LR fractions, 10 μl 1000 U/ml polyethylene glycol superoxide dismutase (PEG-SOD) and 10 μl 3mM NADPH in modified Kreb's/HEPEs buffer for 10 min (total volume is adjusted to 90 μl using Kreb's/HEPEs buffer).
8. After incubation, add 10 μl 10 mM CMH to 90 μl reaction mixture from step 7.
9. 50 μl from step 8 is transferred to a 50 μl capillary tube immediately and analyzed in an ESR spectrometer by time scan to quantify $O_2^{\cdot -}$.
10. A time scan of CMH oxidation is recorded and normalized to the protein content of the sample. $O_2^{\cdot -}$ production from LRs is calculated as the SOD-inhibitable fraction of CMH oxidation.

3.5. Results

To better help readers to understand these methods and design necessary experiments in their studies on LR signaling platforms and redox regulation of cell function, we used FasL-induced formation of LR-redox signaling platforms as example to illustrate some representative results.

3.5.1. FasL-Induced FRET between Rac1 and LR Component

FRET can be detected by confocal microscopy between a fluorophore, FITC as donor and TRITC as acceptor, which shares the character to allow FRET. Acceptor (TRITC) bleaching protocol was applied to calculate the FRET efficiency. Representative images of FRET analysis between FITC-Rac1 (one of NADPH oxidase subunits) and TRITC-CTXB in BCAECs are shown in **Fig. 1b**. The left group of images shows a control cell costained

with FITC-Rac1 and TRITC-CTXB that underwent an acceptor bleaching protocol. Both the pre- and postbleaching images were presented on the top and middle panels. FRET image (in blue) was generated by subtraction of fluorescent intensity in the prebleaching image from that in the postbleaching image of FITC-Rac1 labeling. As shown in FRET image (blue in the bottom image), there was very low FRET detected under control condition. The right group of images shows a FasL-stimulated cell that underwent the same FRET protocol. In addition to detected patch formation (LR clustering and Rac aggregation) and colocalization of both molecules seen in the overlaid images (top panel) in response to FasL, a more intense FRET image (blue one the bottom) was detected in this FasL-treated BCAEC, demonstrating that energy transfer occurs between a Rac1 and LR component-GM1 ganglioside.

3.5.2. Isolation of LR fractions by Flotation Assay

Flotation of DRMs is used to identify redox signaling molecules or other associated proteins and receptors in isolated LRs fractions. The LR fraction was located at the interface between 5% and 30% density gradient fractions in the ultracentrifuge tube after centrifugation (**Fig. 1c**).

3.5.3. FasL-Induced gp91^{phox} Aggregation in LR fractions

In **Fig. 1d**, Western blot analysis showed a positive expression of flotillin-1 in fractions 3–5 (from top to bottom), which was referred to LR fractions. NADPH oxidase subunit, gp91^{phox} can be detected in most of the membrane fractions from BCAECs. However, there was a distribution change among these fractions with a marked increase in gp91^{phox} protein in LR fractions when BCAECs were stimulated by FasL.

3.5.4. FasL-Enhanced NADPH Oxidase Activity

NADPH oxidase activity was detected by measurement of $O_2^{\cdot-}$ production in isolated LR-enriched fractions using ESR. Representative ESR spectra were shown in **Fig. 1e** indicating SOD-inhibitable $O_2^{\cdot-}$ signals (upper) and summarized data for $O_2^{\cdot-}$ production (bottom) indicating that FasL significantly increased $O_2^{\cdot-}$ production in LR fractions.

4. Notes

1. Preparation: Mix 0.4 g PFA in 1.0 ml dH_2O and add 100 µl 1 M NaOH. Then heat this mixture until the PFA is dissolved. Finally, dilute the solution to 10 ml with PBS.
2. OptiPrep® Density Gradient Medium is used for the isolation of cells and cell organelles, which contains 60% (w/v) solution of iodixanol in sterlized water. Gradient sucrose buffer is also commonly used for LR isolation.

3. The concentration of detergent Triton X-100 can be variable (1–2%) based on different cells or tissues. Other detergents such as Brij-96 may be also used.
4. Other spin trap agents specific for superoxide such as DMPO (5,5-dimethyl-1-pyrolline-*N*-oxide), DEPMPO (5-diethoxyphosphoryl-5-1-pyrroline-*N*-oxide), DPPM-DPO (5-(diphenylphosphinoyl)-5-methyl-4,5-dihydro-3H-pyrrole *N*-oxide) are also used in this study.
5. Deferoxamine and DETC are used as metal chelators to decrease CMH background.
6. Isolation of BCAECs is based on the reference *(23)*.
7. Split and culture cells based on common laboratory procedures.
8. All remaining steps are performed in the dark to protect fluorescent signals.
9. Green fluorescence (Alexa 488/FITC) should be paired with Red/Orange fluorescence (Texas Red/TRITC/Alexa 555), and vice versa.
10. The patch formation of Alexa 488-labeled CTX and gangliosides complex represents the clusters of LRs. Clustering is defined as one or several intense spots of fluorescence on the cell surface, whereas unstimulated cells display a homogenous distribution of fluorescence throughout the membrane. In each experiment, the presence or absence of clustering of 200 cells in each sample is scored by three independent observers. The results are given as the percentage of cells showing a cluster after the indicated treatment as described. Similar analysis is also used to summarize target proteins with LRs colocalization.
11. Starting with this step, the followings are FRET visualization-acceptor bleaching procedures. Donor control images are observed under donor excitation/emission wavelengths; Acceptor control images are observed under acceptor excitation/emission wavelengths; FRET control images are observed under donor excitation/acceptor emission wavelengths.
12. The FRET efficiency is calculated through the following formula:

$$E = \frac{\mathrm{FITC}_{\mathrm{post}} - \mathrm{FITC}_{\mathrm{pre}}}{\mathrm{FITC}_{\mathrm{post}}} \times 100\%$$

13. All steps except cell culture and treatment should be performed on ice, preferably in a cold room set at or below 4°C.
14. In this protocol, gradient solution is 40%, 30%, and 5%, each fraction volume is 4.5 ml. This gradient concentration and fraction volume may be adjusted based on different cells and other factors.

15. Alternative centrifuge rotors may be used, the rotor speed RPM need to be adjusted based on different rotors.
16. The number of aliquot fractions may be adjusted.
17. For immunoblot analysis, if protein concentration of each fraction is too low to detect the signal, the proteins of each fraction may be precipitated by mixing with equal volume of 30% trichloroacetic acid and 30 min of incubation on ice. Proteins then spin down by centrifugation at 13,000 × *g* at 4°C for 15 min. The protein pellet is carefully washed with cold acetone twice, air dried, and then resuspended in suitable volume of 1 M Tris-HCl (pH 8.0), which are ready for immunoblot analysis.
18. Western blot analysis is based on common laboratory procedures.
19. Total reaction volume is 100 μl.
20. This measurement is considered as CMH background or baseline. The ESR settings are as follows: biofield, 3,350; field sweep, 60 G; microwave frequency, 9.78 GHz; microwave power, 20 mW; modulation amplitude, 3 G; 4,096 points of resolution; receiver gain, 100; and kinetic time, 10. These settings may be adjusted based on the signals.
21. From steps 4 to 9, LR fractions are prepared and incubated with NADPH and the spin probe CMH in the presence or absence of PEG-SOD.

Acknowledgments

The studies cited in this chapter were supported by grants from the National Institutes of Health (HL-57244, HL-70726, and HL-51055). The content of this publication does not necessarily reflect the views or policies of the Department of Health and Human Services, nor does mention of trade names, commercial products, or organization imply endorsement by the US Government.

References

1. Kabouridis, P.S. (2006) Lipid rafts in T cell receptor signalling. *Mol Membr Biol* **23**: 49–57.
2. Simons, K., and Toomre, D. (2000) Lipid rafts and signal transduction. *Nat Rev Mol Cell Biol* **1**:31–39.
3. Hawkes, D.J., and Mak, J. (2006) Lipid membrane; a novel target for viral and bacterial pathogens. *Curr Drug Targets* **7**:1615–1621.
4. Gulbins, E., and Grassme, H. (2002) Ceramide and cell death receptor clustering. *Biochim Biophys Acta* **1585**:139–145.

5. Li, P.L., Zhang, Y., and Yi, F. (2007) Lipid raft redox signaling platforms in endothelial dysfunction. *Antioxid Redox Signal* **9**: 1457–1470.
6. Jacobson, K., Mouritsen, O.G., and Anderson, R.G. (2007) Lipid rafts: at a crossroad between cell biology and physics. *Nat Cell Biol* **9**:7–14.
7. Allen, J.A., Halverson-Tamboli, R.A., and Rasenick, M.M. (2007) Lipid raft microdomains and neurotransmitter signalling. *Nat Rev Neurosci* **8**:128–140.
8. Zhang, A.Y., Yi, F., Zhang, G., Gulbins, E., and Li, P.L. (2006) Lipid raft clustering and redox signaling platform formation in coronary arterial endothelial cells. *Hypertension* **47**:74–80.
9. Zuo, L., Ushio-Fukai, M., Ikeda, S., Hilenski, L., Patrushev, N., and Alexander, R.W. (2005) Caveolin-1 is essential for activation of Rac1 and NAD(P)H oxidase after angiotensin II type 1 receptor stimulation in vascular smooth muscle cells: role in redox signaling and vascular hypertrophy. *Arterioscler Thromb Vasc Biol* **25**:1824–1830.
10. Touyz, R.M. (2006) Lipid rafts take center stage in endothelial cell redox signaling by death receptors. *Hypertension* **47**:16–18.
11. Bedard, K., and Krause, K.H. (2007) The NOX family of ROS-generating NADPH oxidases: physiology and pathophysiology. *Physiol Rev* **87**:245–313.
12. Ushio-Fukai, M. (2006) Redox signaling in angiogenesis: role of NADPH oxidase. *Cardiovasc Res* **71**:226–235.
13. Bokoch, G.M., and Zhao, T. (2006) Regulation of the phagocyte NADPH oxidase by Rac GTPase. *Antioxid Redox Signal* **8**:1533–1548.
14. Takeya, R., and Sumimoto, H. (2006) Regulation of novel superoxide-producing NAD(P)H oxidases. *Antioxid Redox Signal* **8**:1523–1532.
15. Jin, S., Yi, F., and Li, P.L. (2007) Contribution of lysosomal vesicles to the formation of lipid raft redox signaling platforms in endothelial cells. *Antioxid Redox Signal* **9**:1417–1426.
16. Jin, S., Zhang, Y., Yi, F., and Li, P.L. (2008) Critical role of lipid raft redox signaling platforms in endostatin-induced coronary endothelial dysfunction. *Arterioscler Thromb Vasc Biol* **28**: 485–490.
17. Schmitz, G., and Grandl, M. (2007) Role of redox regulation and lipid rafts in macrophages during Ox-LDL-mediated foam cell formation. *Antioxid Redox Signal* **9**:1499–1518.
18. Grassme, H., Jekle, A., Riehle, A., Schwarz, H., Berger, J., Sandhoff, K., Kolesnick, R., and Gulbins, E. (2001) CD95 signaling via ceramide-rich membrane rafts. *J Biol Chem* **276**: 20589–20596.
19. Sekar, R.B., and Periasamy, A. (2003) Fluorescence resonance energy transfer (FRET) microscopy imaging of live cell protein localizations. *J Cell Biol* **160**:629–633.
20. Sowa, G., Pypaert, M., and Sessa, W.C. (2001) Distinction between signaling mechanisms in lipid rafts vs. caveolae. *Proc Natl Acad Sci U S A* **98**:14072–14077.
21. MacLellan, D.L., Steen, H., Adam, R.M., Garlick, M., Zurakowski, D., Gygi, S.P., Freeman, M.R., and Solomon, K.R. (2005) A quantitative proteomic analysis of growth factor-induced compositional changes in lipid rafts of human smooth muscle cells. *Proteomics* **5**:4733–4742.
22. Hwang, J., Kleinhenz, D.J., Lassegue, B., Griendling, K.K., Dikalov, S., and Hart, C.M. (2005) Peroxisome proliferator-activated receptor-gamma ligands regulate endothelial membrane superoxide production. *Am J Physiol Cell Physiol* **288**:C899–905.
23. Zhang, D.X., Yi, F.X., Zou, A.P., and Li, P.L. (2002) Role of ceramide in TNF-alpha-induced impairment of endothelium-dependent vasorelaxation in coronary arteries. *Am J Physiol Heart Circ Physiol* **283**:H1785–1794.